AIP ADVANCES **5**, 047141 (2015)

Geometrical and physical conditions for skyrmion stability in a nanowire

C. P. Chui,[1] Fusheng Ma,[2] and Yan Zhou[1,a]
[1]*Department of Physics, The University of Hong Kong, Pokfulam Road, Hong Kong, P. R. China*
[2]*Temasek Laboratories, National University of Singapore, 117604, Singapore*

(Received 1 March 2015; accepted 15 April 2015; published online 24 April 2015)

Skyrmions are promising information carriers in the next-generation storage and transmission devices. Appropriate design of the nanowire that permits the flow of skyrmions is, however, seldom studied. In this work, the geometrical and material parameters have been varied to investigate the favorable conditions for skyrmion formation and stability in a nanowire through micromagnetic simulations. It is found that the minimum planar dimensions have to be satisfied in order to stabilize a skyrmion. Furthermore, the nanowire thickness is also important for establishing a skyrmion. The temperature effect in the competition between the perpendicular magnetic anisotropy (PMA) and the Dzyaloshinskii–Moriya interaction (DMI) limits the skyrmion formation in a well-defined phase. On the other hand, fine tuning of the exchange stiffness and the Gilbert damping constant sustain a specified portion of the phase diagram that allows for skyrmion formation. Our study also indicates that the stabilized magnetization pattern is dependent on the initial skyrmion state. These results shed light on the possible configurations that are suitable for the design of skyrmionic devices. © *2015 Author(s). All article content, except where otherwise noted, is licensed under a Creative Commons Attribution 3.0 Unported License.* [http://dx.doi.org/10.1063/1.4919320]

INTRODUCTION

Skyrmions are attractive candidates of information carriers for future data communication, due to their topologically stable spin textures. The application of skyrmions is even more promising after the discovery of controlling its motion by a low current density, leading to lower Joule heating.[1] Moreover, skyrmions can be arranged in lattice configuration to represent an array of binary digits used for information storage.[2–4]

A number of studies have been devoted to skyrmions stored inside a confined geometry, such as nanowire and nanodisk *etc* for storing and transmitting them.[5–8] Theoretical analysis of chiral symmetry breaking has been started with magnetic films having infinite planar dimensions but confined thickness.[9] Recently, equilibrium magnetization has been studied for rectangular and circular nanostructures.[10] Attempt has been made to model the modulation of the skyrmionic core by controlling the thickness of a nanodisc made of chiral magnets.[11] However, the magnetization at varying physical dimensions has not been investigated yet.

The damping is crucial to magnetization dynamics in controlling the relaxation time of reaching the equilibrium magnetization from its initial state, and in determining the angle of precession of the magnetization. Besides, the exchange interaction is crucial to stabilize the skyrmion.[12] However, the combined effect between these two parameters in the stabilization of a skyrmion is yet to be studied.

In chiral ferromagnets, the Dzyaloshinskii–Moriya interaction[13,14] (DMI) is responsible for establishing the skyrmion structure in the surface regions of a chiral magnet with broken inversion

[a]Correspondence and requests for materials should be addressed to Yan Zhou (yanzhou@hku.hk).

 ©Author(s) 2015

All article content, except where otherwise noted, is licensed under a Creative Commons Attribution 3.0 Unported license. See: http://creativecommons.org/licenses/by/3.0/ Downloaded to IP: 147.8.230.88 On: Fri, 24 Jul 2015 08:13:23

symmetry.[2,15–17] On the other hand, the perpendicular magnetic anisotropy (PMA) is responsible for stabilizing the magnetization in skyrmion state[18] in the absence of an external magnetic field. Furthermore, a higher anisotropy leads to enhanced stability by suppressing the helical state.[19,20] Although strong PMA suppresses the formation of magnetic vortices,[21] the competition between the DMI and the PMA has not been attempted until very recently.[22]

In fact, Ref. 22 has already addressed a number of physical conditions that favor skyrmion stability by means of magnetic phase diagrams. However, the effect of damping and geometrical dimensions on skyrmion stability is lacking. In addition, the temperature effect on the competition between PMA and DMI has not been identified. More importantly, the type of initial skyrmion is not mentioned. Whether the results apply to both Bloch and Néel types are therefore questionable.

In this work, we specify several physical conditions to sustain the skyrmion structure in a magnetic nanowire, thereby providing further insights into the design of the nanowires for efficient transmission of skyrmions. Micromagnetic simulations have been performed for a number of physical conditions in a nanowire in the presence of a skyrmion. The parameters used in the simulations mainly followed from those in Ref. 5, in order to mimic the physical conditions of cobalt.

METHODS

Micromagnetic simulations have been attempted based on the Landau–Lifshitz–Gilbert (LLG) equation governing the magnetization of each simulation cell. The time-and-position-dependent magnetization of each cell is governed by the differential equation

$$\frac{\partial \mathbf{M}(\mathbf{r},t)}{\partial t} = -\frac{\gamma}{1+\alpha^2}\mathbf{M}(\mathbf{r},t)\times\mathbf{H}_{\text{eff}}(\mathbf{r},t) - \frac{\alpha\gamma}{M_{\text{sat}}(1+\alpha^2)}\mathbf{M}(\mathbf{r},t)\times[\mathbf{M}(\mathbf{r},t)\times\mathbf{H}_{\text{eff}}(\mathbf{r},t)]. \quad (1)$$

In Eq. (1), M_{sat} is the saturation magnetization, α is the Gilbert damping constant, γ is the gyromagnetic ratio, H_{eff} is the time-and-position-varying effective magnetic field composed of the demagnetizing field, the external field and the internal field of the materials being considered.

The simulations have been undertaken by using version 3 of MuMax,[23] an open-source computational tool for micromagnetic simulations implemented by graphics processing units (GPU). The basic parameters used in various simulations mainly follow from those used in Ref. 5, which models the material properties of cobalt. Two of the material and dimensional parameters would vary depending on the physical situations being investigated. The two varying parameters are mentioned in the Results section. If the parameters are not varied in the Results section, the saturation magnetization M_{sat} remains fixed at 580 kA/m, the exchange stiffness A_{ex} at 15 pJ/m, the PMA K_{u} at 0.8 MJ/m^3, the DMI strength D_{ex} at 3 mJ/m^2, and the damping constant α at 0.3.

A circular Bloch skyrmion of counterclockwise chirality and downward core polarity has been initially put in the central position of a nanowire of varying length, width and thickness. We also investigate the effects of different initial conditions including a Néel skyrmion with charge -1 and downward polarization. Unless otherwise stated, the nanowire dimensions are fixed at a length of 160 nm, a width of 40 nm and a thickness of 1 nm. No periodic boundary condition (PBC) has been imposed. Regardless of the wire dimensions in each of the studies, the simulation box has been discretized into cells of size $1 \times 1 \times 1$ nm^3. Runge-Kutta method has been employed to solve Eq. (1). For micromagnetic simulation at 300 K, the Heun solver in time step of 4 fs has been employed instead. The total simulation time for each case varies from 1 ns to 20 ns depending on the physical situations being considered.

RESULTS

Finite size effect

In order to determine the effect of geometrical parameters on skyrmion formation, nanowires of varying length (l), width (w), and thickness (t) have been simulated. Both the length and width of the nanowire range from 10 nm to 100 nm, whereas the thickness is fixed to be 1 nm, 2 nm, 3 nm,

All article content, except where otherwise noted, is licensed under a Creative Commons Attribution 3.0 Unported license. See: http://creativecommons.org/licenses/by/3.0/ Downloaded to IP: 147.8.230.88 On: Fri, 24 Jul 2015 08:13:23

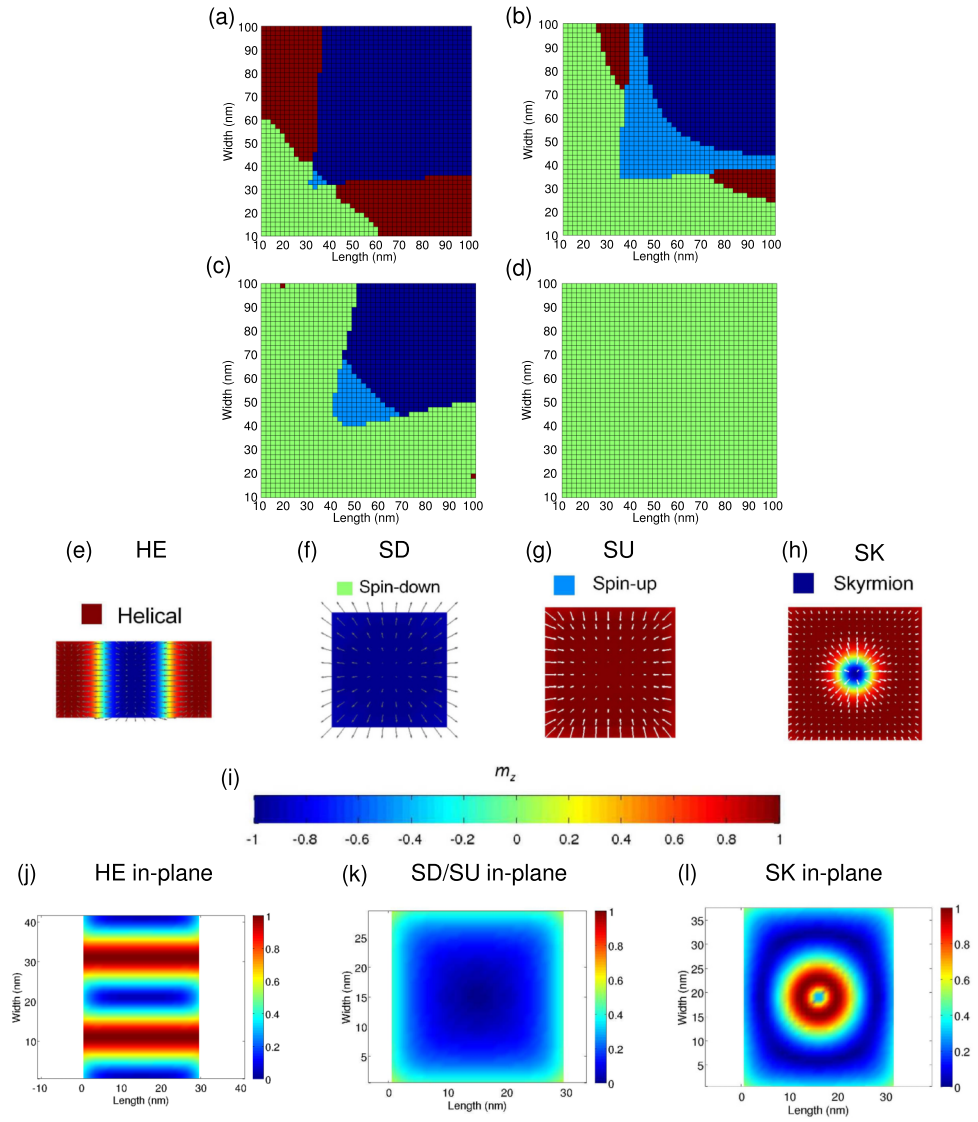

FIG. 1. $l-w$ phase diagrams for thickness equal to (a) 1 nm, (b) 2 nm, (c) 3 nm, and (d) 4 nm, respectively. Four states have been formed: HE (red), SD (pale green), SU (pale blue), and SK (dark blue). (e)–(h) The legend of various out-of-plane magnetization (m_z) patterns obtained from the $l-w$ phase diagram, with arrows indicating the in-plane component of magnetization. (i) The color bar of m_z. (j)–(l) In-plane component of magnetization in color scale for various magnetic phases obtained from Fig. 1(a).

and 4 nm, respectively. A Bloch skyrmion configuration of counterclockwise chirality and downward core polarity is put in the center of the nanowire as the initial magnetization. The material parameters are listed in the Methods section.

The $l-w$ phase diagrams with t = 1 to 4 nm are shown in Fig. 1(a)–1(d), respectively. In each of these subfigures, the red phase is the helical state (HE), pale green the spin-down (SD) state, pale blue the spin-up (SU) state, and dark blue the skyrmion (SK) state. The out-of-plane magnetization m_z of each state is presented in Fig. 1(e)–1(h), whereas the color bar of m_z is shown in Fig. 1(i). Since both the PMA and DMI are of interfacial origin for the structure considered in this study, these two magnetic properties should be scaled with 1/(Co thickness). Therefore, PMA and DMI values are inversely proportional to the thickness in Fig. 1. The equilibrium skyrmion state has changed from the Bloch type (vortex structure) to the Néel type (radially oriented spin texture) (see Fig. 1(h)). Some observations can be inferred from the diagrams. First, the minimum length

All article content, except where otherwise noted, is licensed under a Creative Commons Attribution 3.0 Unported license. See: http://creativecommons.org/licenses/by/3.0/ Downloaded to IP: 147.8.230.88 On: Fri, 24 Jul 2015 08:13:23

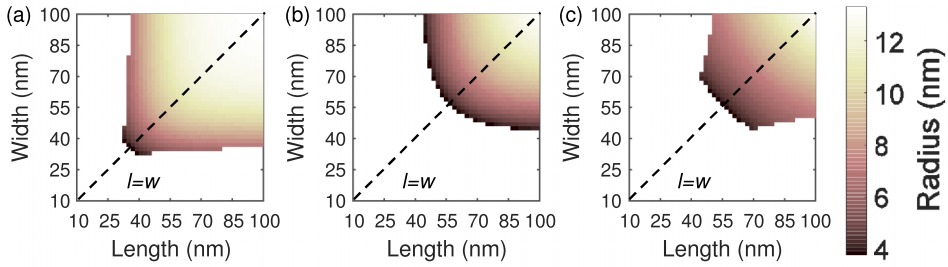

FIG. 2. Radius along the length dimension, for thickness t equal to (a) 1 nm, (b) 2 nm, and (c) 3 nm, respectively. The color bar shows the radius in nm, which is defined as the distance between the skyrmion core and the region where $m_z = 0$. The results are symmetric with respect to the diagonal $l = w$, reflecting the interchangeability of the length and width.

and width required for skyrmion formation increase with increasing thickness. It is noted that a nanowire of t = 4 nm cannot result in stabilized skyrmions; only the SD state remains at the end. Second, the HE phase region is strongly reduced by increasing thickness. In other words, a relatively thick nanowire discourages the stability of both skyrmion and helical state. The simulation results demonstrate the dilution effect of skyrmion formation as a result of increased thickness.

The in-plane magnetization of the four states obtained from the $l - w$ phase diagram are portrayed in Fig. 1(j)–1(l). According to our color scale from 0 to 1, the in-plane magnetization can provide a better indication of the edge effect. The skyrmion growth seems to be constrained by the nanowire edges, at which a rather large in-plane magnetization opposes the expansion of the magnetic vortex perimeter (see Fig. 1(l)). Such a bending of the edge magnetization is induced by the DMI, and has already been derived,[24] supporting the simulation results.

Fig. 2(a) through 2(c) show the radius of the skyrmions that can be formed at thickness t = 1, 2, and 3 nm, respectively. Here, the radius is defined as the distance between the skyrmion core and the region where the out-of-plane magnetization is zero, *i.e.* m_z = 0. As indicated by the color bars, a thicker nanowire can return a skyrmion of larger radius. We have checked the semi-major axes and the semi-minor axes of the skyrmions, and we found the two values are very close such that the skyrmions can be treated as circular.

The equilibrium magnetization represents one of the energy minima of the magnetization phase phase, because it is dependent on the initial conditions used to initiate the simulations. Both larger Bloch skyrmions and Néel skyrmions have been attempted, which lead to different minimum dimensions for skyrmion stability. The change in initial conditions is found to cause variations in the equilibrium magnetization, as indicated by the $l - w$ phase diagrams in Fig. 3. Fig. 3(a) indicates that an initially larger Bloch skyrmion requires even larger geometrical dimensions to stabilize. On the other hand, Fig. 3(b) shows that an initial Néel skyrmion can result in a similar phase diagram as that originated from a Bloch skyrmion in Fig. 1(a). The corresponding radius of stabilized skyrmions are shown in Fig. 3(c) and 3(d), respectively, demonstrating that the resulting radius is also a function of the initial conditions.

Competition between PMA and DMI

The PMA K_u favors vertical alignment of magnetization, while the DMI D_{ex} promotes vortex establishment by orienting the magnetization along the surface. It is thus expected that a balance of these two parameters must be required for the skyrmion stability in a nanowire.

In this section, K_u ranges from 0 to 2 MJ/m^3 in steps of 0.1 MJ/m^2, whereas D_{ex} ranges from 0 to 9 mJ/m^2 in steps of 0.5 mJ/m^2. Other material parameters and the nanowire dimensions are fixed at those values in the Methods section.

We also expect that the initial magnetization would have an effect on the $K_u - D_{ex}$ phase diagrams. Different initial conditions have been attempted to realize their effect on the $K_u - D_{ex}$ phase diagrams shown in Ref. 22. Fig. 4 shows the $K_u - D_{ex}$ phase diagrams for larger initial Bloch skyrmions and Néel skyrmions, respectively. The orange part corresponds to the in-plane

All article content, except where otherwise noted, is licensed under a Creative Commons Attribution 3.0 Unported license. See: http://creativecommons.org/licenses/by/3.0/ Downloaded to IP: 147.8.230.88 On: Fri, 24 Jul 2015 08:13:23

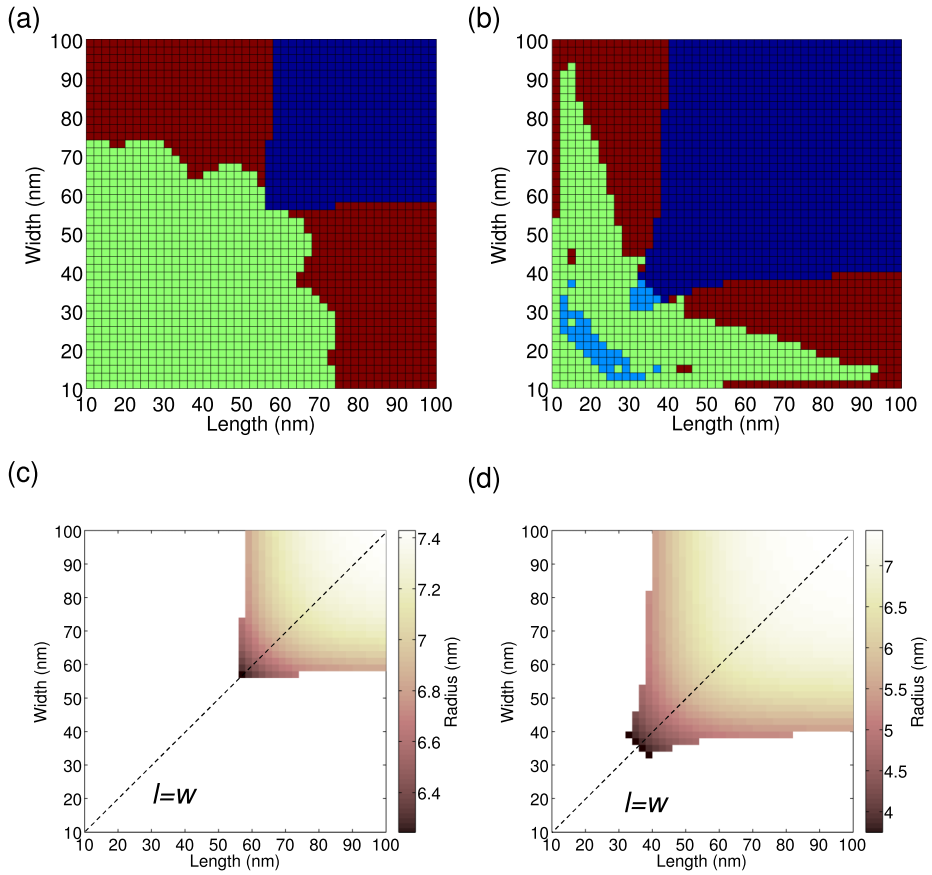

FIG. 3. (a) The phase diagram starting from a Bloch skyrmion with twice the radius as the ones used in Fig. 1. The nanowire thickness is 1 nm. (b) The phase diagram starting from a Néel skyrmion with charge -1 and downward polarization. The nanowire thickness is also 1 nm. The phase points share the same color scheme as those in Fig. 1(e)–1(h). (c) Stabilized skyrmion radius obtained from 3(a). (d) Stabilized skyrmion radius obtained from 3(b). The skyrmions obtained by these two initial conditions are circular.

magnetization (IP), the pale green part the ferromagnetic phase with all spins down (SD), the pale blue part the spin-up state (SU), the dark blue region the skyrmion phase (SK), and the red part is the helical (HE) structure. One can observe that a larger Bloch skyrmion cannot be stabilized for the given ranges of K_u and D_{ex}. However, an initial Néel skyrmion can lead to stabilized skyrmions. It is found that a larger Bloch skyrmion results in a more prominent change in the phase diagram than a Néel skyrmion does.

It is noticed that the dipolar field has minimal effect on the stability of skyrmions. Fig. 4(c) is the magnetic phase diagram obtained by repeating Fig. 4(b) but without considering the dipolar field. By comparing the SK phase regions of these two diagrams, one can realize that the absence of the dipolar field can slightly promote the SK phase and inhibit the HE phase in a nanowire with small DMI and small PMA. Moreover, the absence of the dipolar field can promote the SU state and inhibit the IP phases under small DMI and small PMA. The preference of IP phase in the presence of the dipolar field is attributed by the demagnetizing field along the thickness of a nanowire, which exhibits a higher shape anisotropy.[25]

Fig. 5(a) through 5(c) show the $K_u - D_{ex}$ phase diagrams at room temperature (300 K) after 4 ns, 10 ns, and 20 ns, respectively. The same color scheme in Fig. 4(c) applies here. The skyrmion phase region at room temperature shrinks with time. Part of the skyrmion phase that exists near the SU-SK and HE-SK boundary in Fig. 2(a) of Ref. 22 have changed to the SU and HE state, respectively. Fig. 6(a) through 6(i) display the out-of-plane magnetization m_z of three representative phase points: $(D_{ex}, K_u) = (4.5, 1.4)$, $(D_{ex}, K_u) = (4.5, 1.5)$ and $(D_{ex}, K_u) = (6.0, 1.9)$. The first phase

All article content, except where otherwise noted, is licensed under a Creative Commons Attribution 3.0 Unported license. See: http://creativecommons.org/licenses/by/3.0/ Downloaded to IP: 147.8.230.88 On: Fri, 24 Jul 2015 08:13:23

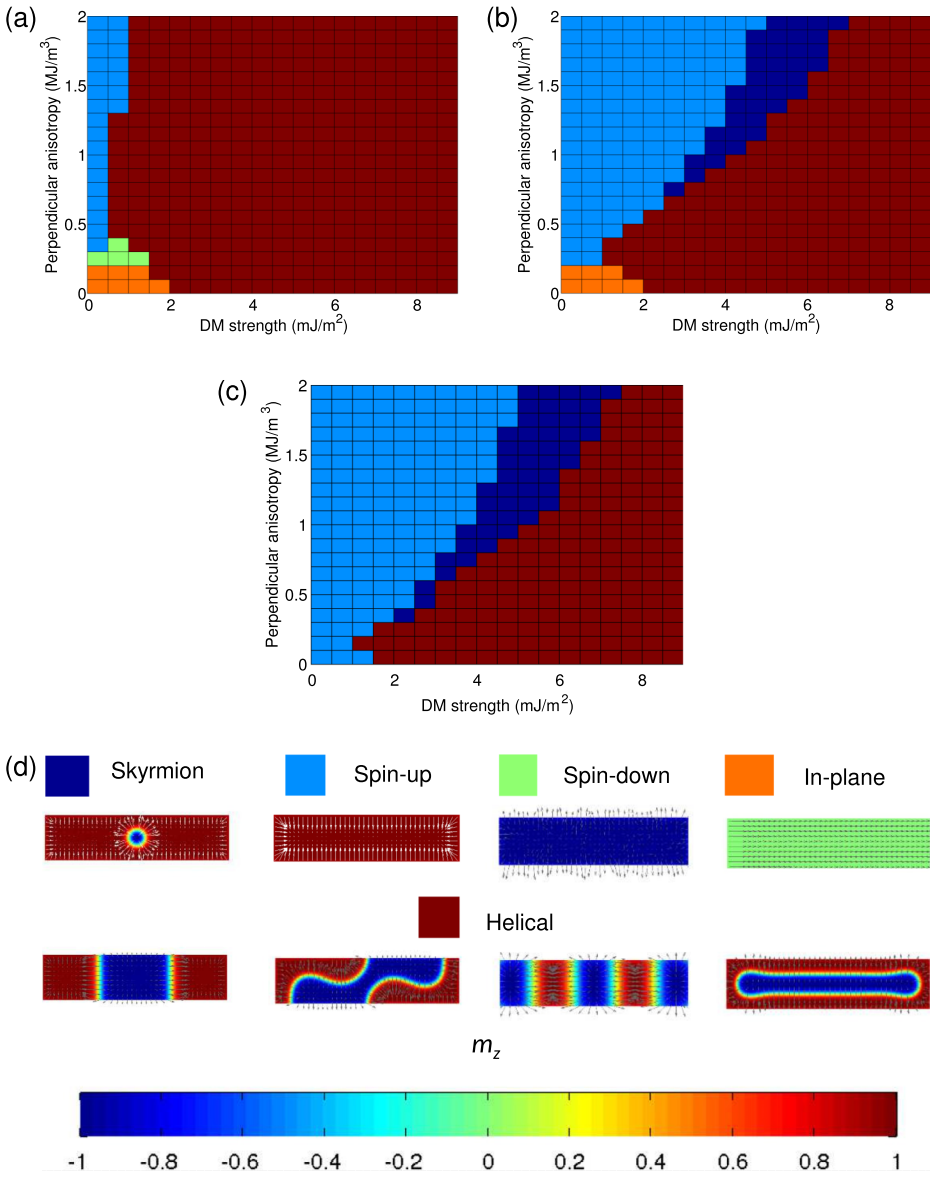

FIG. 4. (a) $K_u - D_{ex}$ phase diagrams arising from initial Bloch skyrmions having radius of 2 units. No skyrmions can be stabilized for the given K_u and D_{ex} ranges. (b) $K_u - D_{ex}$ phase diagrams arising from initial Néel skyrmion of charge -1 and downward polarization. (c) $K_u - D_{ex}$ phase diagram with the same set of parameters as Fig. 4(b) without the dipolar field. (d) The legend of the phase points, with typical m_z plots and the corresponding color bar.

point remains an SK state after 20 ns, while the other two phase points result in SU and HE state after 20 ns. The simulations demonstrate the shrinking of SK phase region as the simulation time is increased at finite temperature. The stabilized skyrmions that can withstand finite temperature for a long simulation time are those with high PMA and DMI.

Competition between exchange interaction and Gilbert damping

The exchange interaction A_{ex} and the Gilbert damping constant α act as another competing pair of factors that would determine the skyrmion stability in a nanowire. Here we investigate the conditions for A_{ex} varying from 0 to 20 pJ/m in steps of 0.5 pJ/m and α from 0.01 to 0.4 in steps of 0.01, with all other material and dimensional parameters fixed at those values mentioned in the Methods section. The resulting $A_{ex} - \alpha$ phase diagram is shown in Fig. 7(a), which shows three phase regions. The red

All article content, except where otherwise noted, is licensed under a Creative Commons Attribution 3.0 Unported license. See: http://creativecommons.org/licenses/by/3.0/ Downloaded to IP: 147.8.230.88 On: Fri, 24 Jul 2015 08:13:23

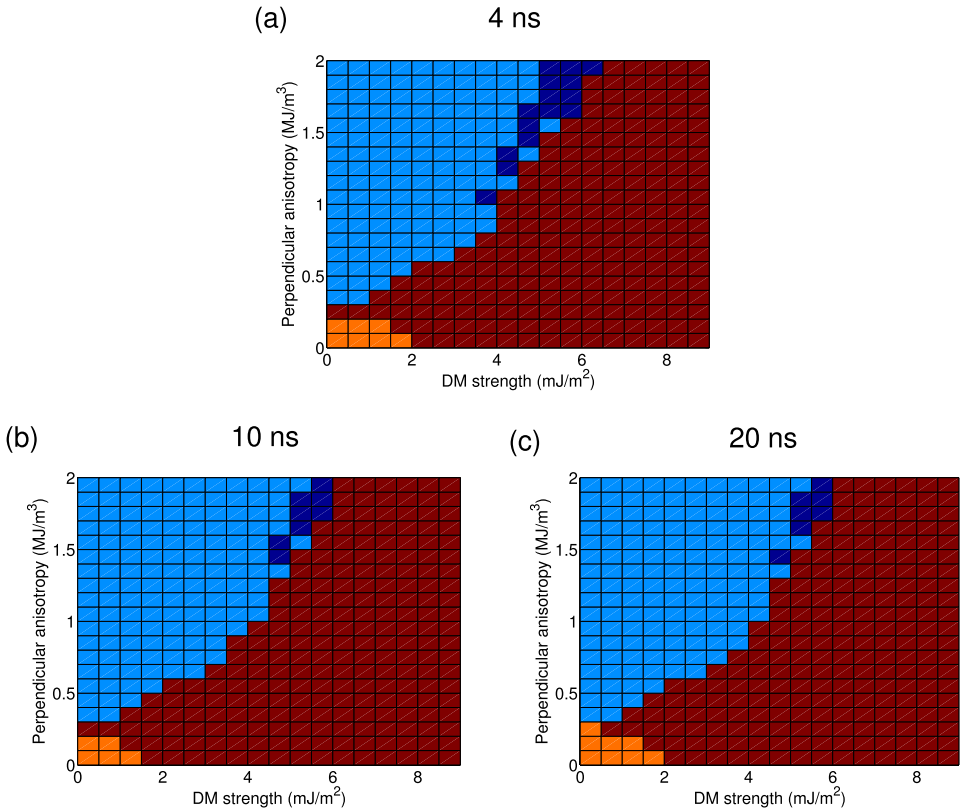

FIG. 5. $K_u - D_{ex}$ phase diagram at 300 K after (a) 4 ns, (b) 10 ns, and (c) 20 ns indicating the decrease in SK phase region with simulation time. The color scheme of phase points follows that of Fig. 4.

region is the DMI phase, the dark blue region is the SK state, the pale blue one is the SU state. The color scheme of Fig. 7(a) follows that of the $K_u - D_{ex}$ phase diagram in Fig. 4. Starting with a Bloch skyrmion as the initial condition, the skyrmions can be formed when the damping constant is at least about 0.12, provided that the exchange stiffness is greater than 8.2 pJ/m. With the variation range of the parameters presented in this work, A_{ex} cannot increase without bound if the skyrmion state has to be maintained; otherwise, a spin-up state would be formed at equilibrium. Nevertheless, it does demonstrate that a large A_{ex} and a large α should be beneficial to the skyrmion stability.

Figs. 7(b) and 7(c) show the semi-major and semi-minor axes of the skyrmions, which indicates the elliptical nature of the skyrmions since the two values are appreciably different. The longer side, *i.e.* the length, would result in the semi-major axis. The stabilized skyrmions are found to be circular along the SU-SK boundary, whereas they are elliptical along the HE-SK boundary. The expansion of a circular skyrmion from its initial state is constrained by the edge effect, in the sense that an elliptical skyrmion is reluctant to become the equilibrium state. Again, the semi-major and semi-minor axes are defined as the distance between the skyrmion core and the region in which $m_z = 0$, each measured along the longer and shorter dimension, respectively.

According to the $A_{ex} - \alpha$ phase diagram, one can regard the skyrmion state as the intermediate state between the helical state and the ferromagnetic state, given that the nanowire dimensions are fixed. As A_{ex} increases, the magnetization of the whole sample would tend to flip toward the same direction which disallows the growth of a skyrmion with winding magnetization. For a skyrmion to be stabilized, an appropriate combination of A_{ex} and α is therefore necessary. Although the thorough understanding of the phase diagram especially the role of damping is lacking, we notice that the minimum damping constant is crucial for the skyrmion stability. This finding is consistent with the results obtained in the literature.[5,26,27] For example, it was numerically demonstrated that isolated skyrmions can be created by circular electric currents and a strong Gilbert damping is

All article content, except where otherwise noted, is licensed under a Creative Commons Attribution 3.0 Unported license. See: http://creativecommons.org/licenses/by/3.0/ Downloaded to IP: 147.8.230.88 On: Fri, 24 Jul 2015 08:13:23

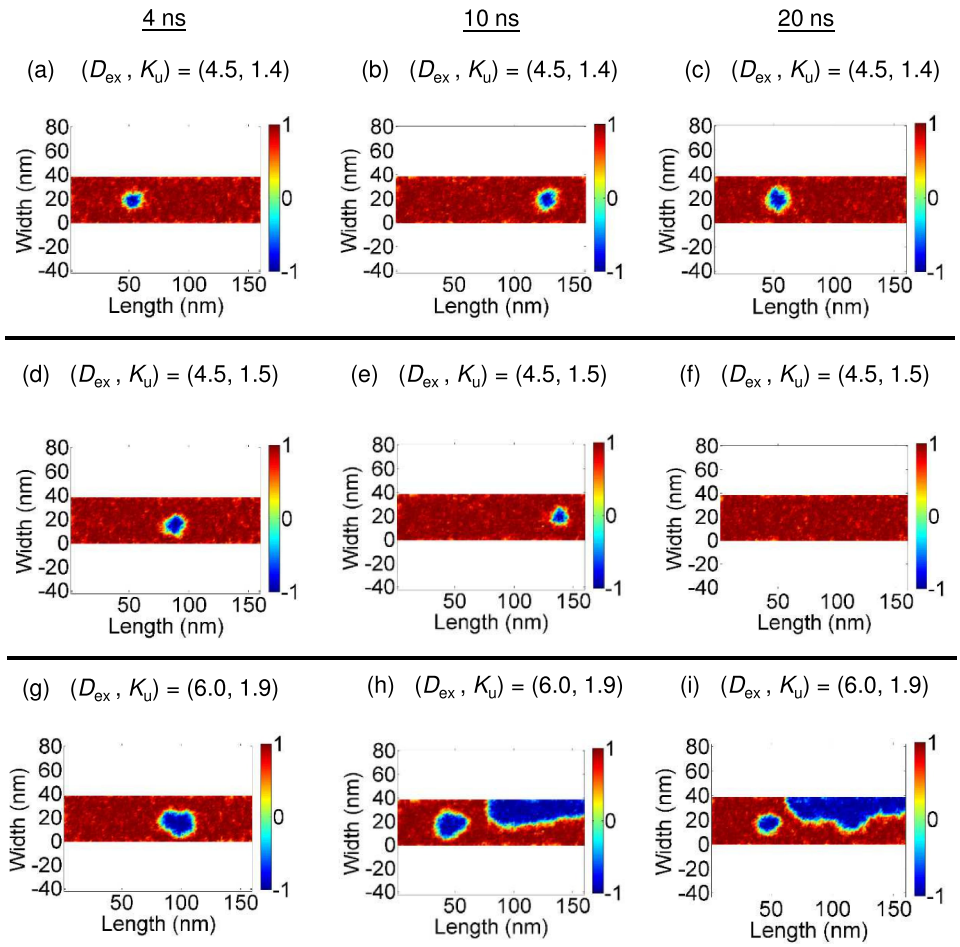

FIG. 6. (a)–(c) Snapshots of out-of-plane magnetization (m_z) for $(D_{ex}, K_u) = (4.5, 1.4)$, ending up with the SK state at 20 ns. (d)–(f) Snapshots of m_z for $(D_{ex}, K_u) = (4.5, 1.5)$, ending up with the SU state at 20 ns. (g)–(i) Snapshots of m_z for $(D_{ex}, K_u) = (6.0, 1.9)$, ending up with the HE state at 20 ns.

crucial to achieve the skyrmion generation in Ref. 26. In addition, it is found that damping plays an important role in dynamical processes of the dynamical skyrmion transformations in Ref. 27 and skyrmion nucleation current in Ref. 5. For damping smaller than a critical value, multi-domain states are more favored than skyrmion. Therefore it is expected that the damping constant contributes to the final nucleation phase diagram, although a detailed understanding is required.

DISCUSSION

According to the $l - w$ phase diagrams in Fig. 1, one can realize the change in magnetization as the planar dimensions increase. As a nanowire has both narrow length and width given fixed thickness, the equilibrium magnetization follows that of the initial vortex core (which is downward in our study). Then the SD state experiences a magnetic reversal to the SU state as both dimensions increase. It means that the equilibrium magnetization of the whole nanowire follows that of the perimeter of the initial state. As both dimensions further increase, a complete winding of the magnetization can be established, thereby forming a skyrmion. The thickness of a nanowire is another issue that determines the skyrmion stability. It can be seen that skyrmion formation is possible in smaller length and width when using a thinner nanowire.

The $l - w$ phase diagrams suggest an approach to control the magnetic state externally during information transmission without changing the materials parameters. It can be inferred that a

All article content, except where otherwise noted, is licensed under a Creative Commons Attribution 3.0 Unported license. See: http://creativecommons.org/licenses/by/3.0/ Downloaded to IP: 147.8.230.88 On: Fri, 24 Jul 2015 08:13:23

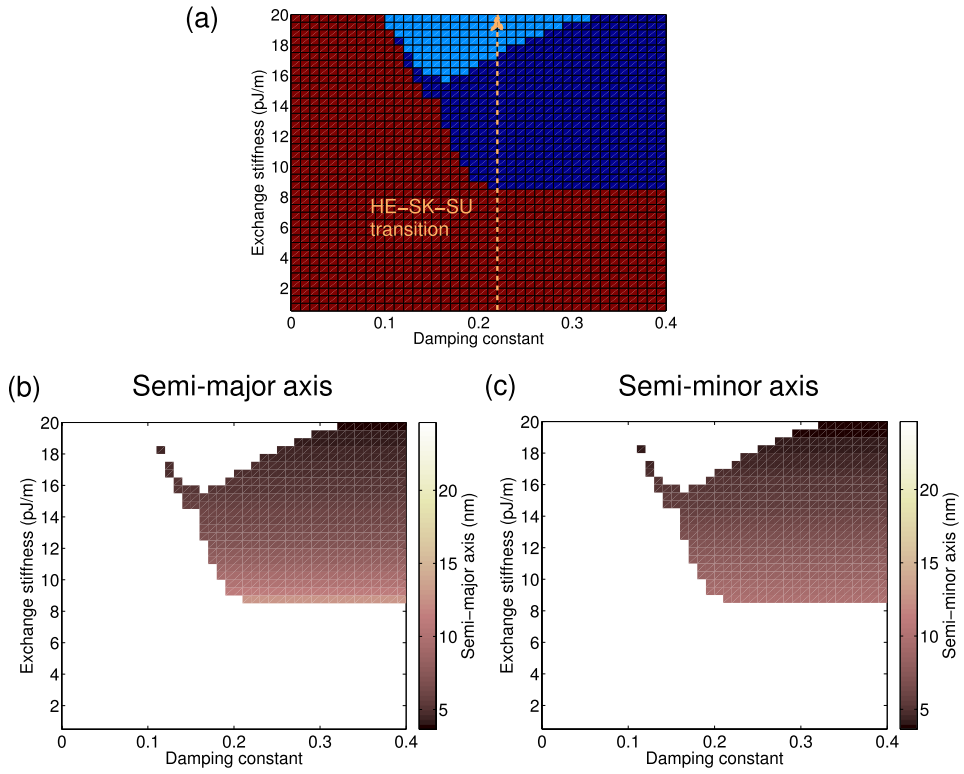

FIG. 7. (a) The $A_{ex} - \alpha$ phase diagram where $0 \le A_{ex} \le 20$ pJ/m and $0.01 \le \alpha \le 0.4$, with HE state (red), SK state (dark blue), and SU state (pale blue). The magnetization patterns obtained in the $A_{ex} - \alpha$ phase diagram follow those obtained in the $K_u - D_{ex}$ phase diagram in Fig. 4. As the DMI is fixed at 3 mJ/m^2, the phase diagram shows the phase transition from HE to SK and finally to SU state as the exchange stiffness increases. (b)–(c) The length of the semi-major axis of the elliptical skyrmion after equilibrium. The skyrmion dimensions decrease with increasing A_{ex} and α.

moving skyrmion entering the narrower portion of a nanowire would experience boundary conditions change. However, our study cannot reveal whether a helical state that is already stabilized in a nanowire can return to a skyrmion as the magnetization encounters a larger planar area again.

The requirement of a large DMI and a large PMA for the stability of skyrmions at absolute zero temperature has already been addressed in Ref. 22. In our study, the finite temperature effect on the $K_u - D_{ex}$ phase diagram reinforces the role of both PMA and DMI in the skyrmion stability. A further increase in DMI and PMA is necessary to stabilize a skyrmion at a finite temperature, without which it would degenerate to other magnetization states.

The $A_{ex} - \alpha$ phase diagram shown in Fig. 7(a) indicates that both large A_{ex} and large α are helpful to skyrmion formation. A large A_{ex} encourages parallel alignment of magnetization in a more confined space. Such a reinforced alignment can be reflected in the shrinking skyrmion size exhibited in Fig. 7(b) and 7(c) as both A_{ex} and α increase.

Additionally, Fig. 7(a) can verify implicitly the competition between exchange stiffness and DMI. First, the phase diagram is obtained at $D_{ex} = 3$ mJ/m^2. As A_{ex} increases from 0 to 20 pJ/m, one can observe the change in phase from HE to SK and finally to SU state. Therefore one can realize that the SK state is an intermediate state between the HE state and the SU state in the course of increasing the exchange stiffness.[28]

CONCLUSION

We have demonstrated several considerations in the design of nanowires used for stabilizing skyrmions. There exists some minimum planar dimensional conditions for the formation of a skyrmion. Reduction to spin-down or spin-up structure is possible by decreasing the planar

All article content, except where otherwise noted, is licensed under a Creative Commons Attribution 3.0 Unported license. See: http://creativecommons.org/licenses/by/3.0/ Downloaded to IP: 147.8.230.88 On: Fri, 24 Jul 2015 08:13:23

dimensions. A further increase in PMA and DMI is necessary for the skyrmion stability at finite temperature. For the competition between the exchange stiffness and the Gilbert damping constant, it is observed that the damping should be rather large to obtain a skyrmion rather than the spin-up state or the helical state. The exchange interaction should also be sufficiently large, but it should be capped to avoid the appearance of the ferromagnetic state. For all these simulations, the initial skyrmion state is crucial for determining the stabilized magnetization state.

ACKNOWLEDGMENTS

Yan Zhou thanks the support by the Seed Funding Program for Basic Research and Seed Funding Program for Applied Research from the University of Hong Kong, ITF Tier 3 funding (ITS/171/13) and University Grants Committee of Hong Kong (Contract No. AoE/P-04/08).

[1] X. Z. Yu, N. Kanazawa, W. Z. Zhang, T. Nagai, T. Hara, K. Kimoto, Y. Matsui, Y. Onose, and Y. Tokura, "Skyrmion flow near room temperature in an ultralow current density," Nat. Commun. **3**, 988 (2012).
[2] S. Mühlbauer, B. Binz, F. Jonietz, C. Pfleiderer, A. Rosch, A. Neubauer, R. Georgii, and P. Böni, "Skyrmion lattice in a chiral magnet," Science **323**, 915–919 (2009).
[3] S. Heinze, K. von Bergmann, M. Menzel, J. Brede, A. Kubetzka, R. Wiesendanger, G. Bihlmayer, and S. Blügel, "Spontaneous atomic-scale magnetic skyrmion lattice in two dimensions," Nature Phys. **7**, 713–718 (2011).
[4] A. Tonomura, X. Yu, K. Yanagisawa, T. Matsuda, Y. Onose, N. Kanazawa, H. S. Park, and Y. Tokura, "Real-space observation of skyrmion lattice in helimagnet MnSi thin samples," Nano Lett. **12**, 1673–1677 (2012).
[5] J. Sampiao, V. Cros, S. Rohart, A. Thiaville, and A. Fert, "Nucleation, stability and current-induced motion of isolated magnetic skyrmions in nanostructures," Nature Nanotech. **8**, 839–844 (2013).
[6] A. Fert, V. Cros, and J. Sampaio, "Skyrmions on the track," Nature Nanotech. **8**, 152–156 (2013).
[7] J. Iwasaki, M. Mochizuki, and N. Nagaosa, "Current-induced skyrmion dynamics in constricted geometries," Nature Nanotech. **8**, 742–747 (2013).
[8] Y. Zhou and M. Ezawa, "A reversible conversion between a skyrmion and a domain-wall pair in a junction geometry," Nature Commun. **5**, 4652 (2014).
[9] A. N. Bogdanov and U. K. Rößler, "Chiral symmetry breaking in magnetic thin films and multilayers," Phys. Rev. Lett. **87**, 037203 (2001).
[10] M. Beg, D. Chernyshenko, M.-A. Bisotti, W. Wang, M. Albert, R. L. Stamps, and H. Fangohr, "Finite size effects, stability, hysteretic behaviour, and reversal mechanism of skyrmionic textures in nanostructures," arXiv:1312.7665v2 (2014).
[11] H. Du, W. Ning, M. Tian, and Y. Zhang, "Magnetic vortex with skyrmionic core in a thin nanodisk of chiral magnets," Europhys. Lett. **101**, 37001 (2013).
[12] Ar. Abanov and V. L. Pokrovsky, "Skyrmion in a real magnetic film," Phys. Rev. B **58**, R8889–R8892.
[13] I. Dzyaloshinskii, "A thermodynamic theory of 'weak' ferromagnetism of antiferromagnetics," J. Phys. Chem. Solids **4**, 241–255 (1958).
[14] T. Moriya, "Anisotropic superexchange interaction and weak ferromagnetism," Phys. Rev. **120**, 91–98 (1960).
[15] X. Z. Yu, Y. Onose, N. Kanazawa, J. H. Park, J. H. Han, Y. Matsui, N. Nagaosa, and Y. Tokura, "Real-space observation of a two-dimensional skyrmion crystal," Nature **465**, 901–904 (2010).
[16] C. Pfleiderer and A. Rosch, "Condensed-matter physics: Single skyrmions spotted," Nature **465**, 880–881 (2010).
[17] C. Pfleiderer, "Magnetic order: Surfaces get hairy," Nature Phys. **7**, 673–674 (2011).
[18] H. Du, J. P. DeGrave, F. Xue, D. Liang, W. Ning, J. Yang, M. Tian, Y. Zhang, and S. Jin, "Highly stable skyrmion state in helimagnetic MnSi nanowires," Nano Lett. **14**, 2026–2032 (2014).
[19] A. B. Butenko, A. A. Leonov, U. K. Rößler, and A. N. Bogdanov, "Stabilization of skyrmion textures by uniaxial distortions in noncentrosymmetric cubic helimagnets," Phys. Rev. B **82**, 052403 (2010).
[20] X. Z. Yu, N. Kanazawa, Y. Onose, K. Kimoto, W. Z. Zhang, S. Ishiwata, Y. Matsui, and Y. Tokura, "Near room-temperature formation of a skyrmion crystal in thin-films of the helimagnet FeGe," Nature Mater. **10**, 106–109 (2011).
[21] M. N. Wilson, A. B. Butenko, A. N. Bogdanov, and T. L. Monchesky, "Chiral skyrmions in cubic helimagnet films: The role of uniaxial anisotropy," Phys. Rev. B **89**, 094411 (2014).
[22] J.-W. Yoo, S.-J. Lee, J.-H. Moon, and K.-J. Lee, "Phase Diagram of a Single Skyrmion in Magnetic Nanowires," IEEE Trans. Magn. **50**, 1500504 (2014).
[23] A. Vansteenkiste, J. Leliaert, M. Dvornik, M. Helsen, F. Garcia-Sanchez, and B. V. Waeyenberge, "The design and verification of MuMax3," AIP Adv. **4**, 107133 (2014).
[24] S. Rohart and A. Thiaville, "Skyrmion confinement in ultrathin film nanostructures in the presence of Dzyaloshinskii–Moriya interaction," Phys. Rev. B **88**, 184422 (2013).
[25] H. Y. Kwon, K. M. Bu, Y. Z. Wu, and C. Won, "Effect of anisotropy and dipole interaction on long-range order magnetic structures generated by Dzyaloshinskii–Moriya interaction," J. Magn. Magn. Mater. **324**, 2171–2176 (2012).
[26] Y. B. Tchoe and J. H. Han, "Skyrmion generation by current," Phys. Rev. B **85**, 174416 (2012).
[27] Y. Zhou, E. Iacocca, A. Awad, R. K. Dumas, F. C. Zhang, H. B. Braun, and J. Åkerman, "Dynamical magnetic skyrmions," arXiv:1404.3281 (2014).
[28] S. Seki, X. Z. Yu, S. Ishiwata, and Y. Tokura, "Observation of skyrmions in a multiferroic material," Science **336**, 198–201 (2012).

All article content, except where otherwise noted, is licensed under a Creative Commons Attribution 3.0 Unported license. See: http://creativecommons.org/licenses/by/3.0/ Downloaded to IP: 147.8.230.88 On: Fri, 24 Jul 2015 08:13:23